

### 3D-FSE Inner Volume Imaging using 3D selective excitation

Shaihan J Malik<sup>1</sup> and Joseph V Hajnal<sup>1,2</sup>

<sup>1</sup>Division of Imaging Sciences and Biomedical Engineering, Kings College London, London, United Kingdom, <sup>2</sup>Centre for the Developing Brain, Kings College London, London, United Kingdom

**Target Audience** Subject specific RF pulse design for use in imaging sequences; new imaging methodology

**Purpose** The 3D Fast Spin Echo sequence offers a very good candidate for inner volume imaging (IVI)<sup>1</sup>, since magnetization that is not transverse after the excitation pulse does not contribute any signal thereafter. Consequently a single (potentially long) multidimensional RF pulse can be employed for localized excitation, followed by a long train of non-selective refocusing pulses thus maintaining short inter-echo spacing. This is the case even for low refocusing flip angles as commonly used with long echo trains. In practise the long durations of multidimensional RF pulses make them susceptible to off-resonance effects, and 2D localization is at the limit of what is achievable with practical pulse durations. Full 3D localization has been achieved using parallel transmission (PTx)<sup>2,3</sup> but it has thus far been attempted for gradient echo imaging in humans; here the duration of the resulting pulses and concerns over SAR are both limiting issues. In this work tailored 3D excitations with built in  $B_0$  compensation have been realised using parallel transmission (PTx) and applied to a standard T2 weighted 3D-FSE protocol in the human brain, yielding large reductions in imaging time with similar image quality to a standard sequence.

**Methods** This work was carried out using a 3T Philips Achieva MRI system fitted with an 8-channel parallel transmit (PTx) body coil<sup>4</sup>. 3D-RF pulses were designed using the linear-class Large Tip Angle (LC-LTA)<sup>5</sup> method formulated in the spatial domain<sup>6</sup> as  $\mathbf{m} = \mathbf{A} \mathbf{b}$  where  $\mathbf{m}(\mathbf{x})$  is the achieved flip angle,  $\mathbf{b}(t)$  is the RF pulse and  $\mathbf{A}$  is the system matrix that describes the effects of both gradient encoding and sensitivity information of each channel. In the case of the CPMG FSE sequence a 90° phase offset must be maintained between excitation and refocusing pulses. By convention we set the phase of the refocusing pulses to 0° so  $\mathbf{m}(\mathbf{x})$  must have phase 90°; i.e.  $\mathbf{m}(\mathbf{x})$  should be imaginary. For general complex  $\mathbf{m}$ ,  $\text{Im}(\mathbf{m})$  creates stable echoes while  $\text{Re}(\mathbf{m})$  produces signals that are suppressed by the CPMG FSE sequence. To take advantage of this idiosyncrasy the problem was rewritten as in Eq.1 and solved as a weighted optimization  $\min\{||\mathbf{Ab}-\mathbf{m}||_w^2 + \lambda||\mathbf{b}||^2\}$ , where a lesser weight ( $W=0.25$ ) was given to  $\text{Re}(\mathbf{m})$  relative to  $\text{Im}(\mathbf{m})$ . This aims to bias excitation errors towards  $\text{Re}(\mathbf{m})$  which are then suppressed by the sequence; a separate abstract has been submitted with further detail on this approach.

In order to create a 3D localized excitation a '3D-shells' k-space trajectory<sup>2</sup> was used. There is currently no tractable systematic way for optimizing such trajectories; instead pilot 3D whole head  $B_1^+$  and  $B_0$  field data were used to optimize heuristically (3D  $B_1^+$  maps were acquired using the AFI<sup>7</sup> method along with low flip angle gradient echo images to obtain per-channel information). The trajectory used had 7 shells with maximum radius 300 rad m<sup>-1</sup> and spacing 50 rad m<sup>-1</sup> giving approximate radial resolution of 10mm and field of view 125mm. It was also found that rotating successive shells by 30° (as shown in Fig.1) was beneficial. Time optimal gradient waveforms were generated using the method of Lustig et al<sup>8</sup> for max. slew rate 180 Tm<sup>-1</sup>s<sup>-1</sup> resulting in duration 12.0ms. A forward model of the system's known gradient performance including delays and eddy currents was used to estimate the true k-space, which was then used in the RF design (Fig.1). In order to limit peak RF power, the iterative reVERSE<sup>9</sup> method was used, and as a result the actual pulse duration differed slightly from subject to subject. A spectrally selective fat suppression pulse was used immediately prior to the excitation, necessary since selectivity at the fat frequency was not controlled.

In-vivo imaging used a standard T2w 3D-FSE protocol with 106 echoes per shot (incl. 6 dummies), TR=2500ms, ESP=4.0ms, asymptotic refocusing flip angle 35°, resolution 1x1x1mm<sup>3</sup>. The Full FOV sequence had FOV 240x240x180mm<sup>3</sup> with SENSE factor 2x2 (an 8-channel head coil was used for reception), scan duration 3m37s; the IVI sequence used FOV 70x70x70mm<sup>3</sup> with no SENSE, duration 1m40s for the same resolution. Note that aside from limiting peak RF power, SAR is not a major concern for this sequence since it runs at only 5% of the 3.2W/kg head average limit and the vast majority of this is contributed by the refocusing pulses, which are delivered using the quadrature mode of the Tx coil (and hence have well characterized SAR).

**Results & Discussion** IVI was successfully achieved in 4 volunteer examinations with custom excitation pulses designed in real time during each session. Results are presented for a target excitation of a cube with width 65mm centred approximately over the cerebellum; optimized pulse duration was 12.4ms. Figure 2 shows the resulting predicted flip angle from the linear design:  $\text{Im}(\mathbf{m})$  shows good predicted background suppression with error concentrated in  $\text{Re}(\mathbf{m})$ . Bloch simulations shows the LC-LTA design performs well though there is some phase deviation within the inner volume region. This could be improved in future by using more advanced LTA design methods. The Full FOV 3D-FSE images shown in Fig.3 demonstrate that the excitation worked as intended with similar contrast in the inner volume region and good suppression outside. Reduced FOV IVI images (Fig 4) have comparable image quality with similar contrast in under half the time.

**Conclusion** We have demonstrated in-vivo IVI using PTx and 3D-FSE imaging with clinically viable parameters using the natural combination of tailored excitation with non-selective refocusing. Though the example given was in the brain, future work may focus on body applications where large time reductions could be achieved when imaging small embedded structures (e.g. the prostate).

**References** 1 Mitsouras et al, Med. Phys. 33, 173–186 (2006). 2. Schneider et al, MRM 69 1369-78 (2013). 3. Haas et al, Proc ISMRM 20, 3764 (2012). 4. Vernickel et al, MRM 58, 381–9 (2007). 5. Pauly et al, JMR 82, 571–587 (1989). 6. Grissom et al, MRM 56, 620–9 (2006). 7 Yarnykh, MRM 57, 192–200 (2007). 8. Lustig et al, IEEE-TMI 27, 866–873 (2008). 9. Lee et al, MRM 67, 353–62 (2012).

$$\begin{bmatrix} \text{Im}(\mathbf{A}) & \text{Re}(\mathbf{A}) \\ \text{Re}(\mathbf{A}) & -\text{Im}(\mathbf{A}) \end{bmatrix} \times \begin{bmatrix} \text{Re}(\mathbf{b}) \\ \text{Im}(\mathbf{b}) \end{bmatrix} = \begin{bmatrix} \text{Im}(\mathbf{m}) \\ \text{Re}(\mathbf{m}) \end{bmatrix} \quad \text{Eq.1}$$

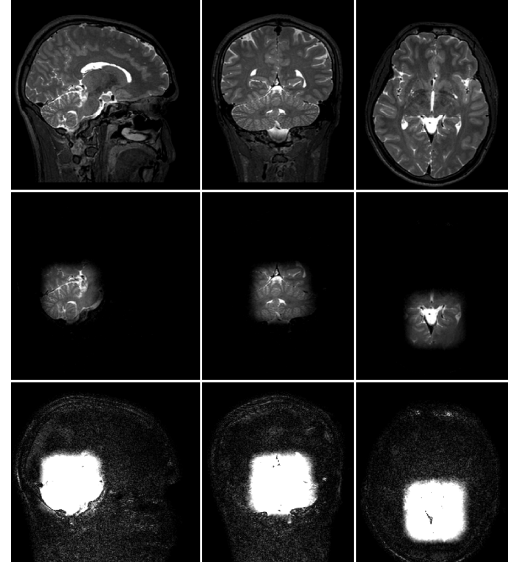
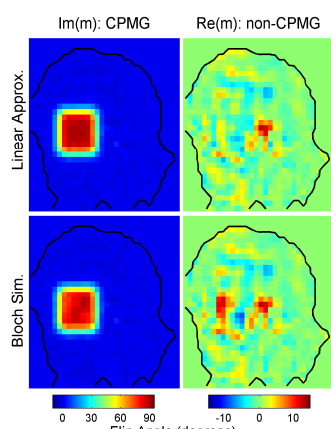
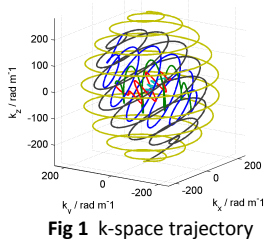


Fig 3 In-vivo full FOV 3D-FSE. Top: non-selective excitation (reference). Middle: IVI with same display settings. Bottom: IVI with windowing display background

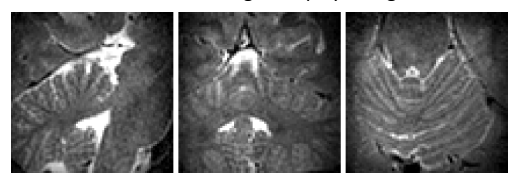


Fig 4 In-vivo IVI 3D-FSE with reduced FOV encoding